P4.3 IMPLEMENTATION OF A DUAL-MODE CLOUD DROPLET SPECTRUM AND PROGNOSTIC NUMBER CONCENTRATION OF CLOUD DROPLETS IN THE CSU-RAMS MODEL

Stephen M. Saleeby *
Colorado State University, Ft. Collins, Colorado

William R. Cotton
Colorado State University, Ft. Collins, Colorado

1. INTRODUCTION

A second cloud mode of large cloud droplets with diameters from 40-80 micron and prediction of cloud droplet number concentration has been implemented in the Colorado State University - Regional Atmospheric Modeling System (CSU-RAMS). The new large cloud droplet mode, in combination with the traditional single mode of cloud droplets, allows for a more accurate representation of the bi-modal distribution of cloud droplets that occurs in the atmosphere. The introduction of prognostic number concentration of cloud droplets, via nucleation of cloud condensation nuclei (CCN), provides a more precise calculation of the amount of droplet mass and number, and it also limits the amount of nucleated cloud water depending upon available CCN.

The new droplet category joins the other seven hydrometeor species that are accounted for in RAMS. These are: small cloud droplets, large cloud droplets, rain, pristine ice, snow, aggregates, graupel, and hail. The large cloud droplet mode (hereafter referred to as "cloud2") is allowed to interact with all other species, similar to the small droplet mode (hereafter referred to as "cloud1"). Cloud2 plays a significant role in the collision–coalescence process by requiring droplets to grow at a somewhat slower rate as they pass from cloud1 to cloud2 to rain. There is also a significant impact by cloud2 upon ice formation, since two modes now exist and are allowed to participate in homogenous freezing nucleation and collisions with ice species. The combination of the two modes contains more cloud water mass than the previous single cloud category; this extra mass also has the potential of influencing the impact of the Hallett-Mossop secondary ice production process and the amount of mass in the pristine ice category as well.

Along with the addition of cloud2, the prognosis of number concentration of both cloud modes has been introduced. This was made possible through use of a Lagrangian parcel model, which is discussed in Feingold and Heymsfield (1992). The parcel model has made it possible to construct lookup tables, for use in RAMS' cloud droplet nucleation routine, that predict the percent of CCN to activate depending upon model atmospheric conditions. CCN are presumed to be ammonium sulfate particles that nucleate into cloud1, and giant cloud condensation nuclei (GCCN) are assumed to consist of sodium chloride particles that nucleate into cloud2. Preliminary tests have been performed for homogeneous supercell simulations that are initiated with a convective sounding and warm bubble. Preliminary results reveal several significant differences in storm development depending upon the initial CCN and GCCN fields that are user-specified. Further tests will be performed for icing, fog, and stratus events to determine the overall impact of the second cloud mode and prediction of droplet number concentration from CCN and GCCN.

Corresponding author address: Stephen M. Saleeby, Atmospheric Sci Dept., Colorado State Univ, Fort Collins, CO 80523; e-mail: smsaleeb@atmos.colostate.edu

2. LAGRANGIAN PARCEL MODEL

The Lagrangian parcel model (Feingold and Heymsfield, 1992) approach used in prediction of cloud droplet nucleation follows the Kohler equations found in Prupacher and Klett (1997). The current application uses a bi-modal spectrum of CCN and GCCN with mass ranges from 10^{-17} kg to 10^{-8} kg. The CCN distribution is comprised of ammonium sulfate particles with a median radius of 0.04 microns, and the GCCN have a sodium chloride composition with a median radius of 3 microns. The original parcel model included ammomium sulfate as the only option for specifying CCN chemical composition. Sodium chloride was introduced in the parcel model as an additional option; information on the molality and Van't Hoff factor was provided by Kunkel (1969).

The lookup table approach, used to adapt the parcel model to the RAMS model, considers the percentage of CCN and GCCN that nucleate into droplets, depending upon the initial user-specified nuclei spectrum and ambient environmental conditions. Parcel model tests have shown strong dependence upon temperature, vertical velocity, and initial concentrations of CCN and GCCN. For the sake of minimizing the number of dimensions in the lookup tables, constants were used for the nuceli median radius, log-normal distribution

breadth parameter, and atmospheric pressure. Compared to the other ambient variables, model results varied the least over a typical range of pressure levels and distribution breadth parameters. The parcel model also assumes that given parcels reach supersaturation before nucleating excess vapor. Tests of various initial saturation values from 85% to 99% show small variances in the final percentage of activated CCN compared to the dependence of the variables mentioned above.

From these tests, 3D and 4D lookup tables were created for single and bi-modal nuclei distributions, respectively. RAMS linearly interpolates between table values for a CCN concentration range of 10 – 10000 (#/cm^3), GCCN from 10^{-6} to 10^{-1} (#/cm^3), vertical velocity from 1 – 10000 cm/s, and temperature from –30C to 30C; pressure is fixed at 600mb.

The parcel model was run until saturation was reached for every combination of the above parameters at various intervals, and lookup tables were produced which contain the percent of available CCN and GCCN to nucleate in RAMS. The amount of excess vapor in RAMS is split between the CCN and GCCN categories depending upon the ratio of the mixing ratio of the CCN and GCCN categories in the parcel model, meaning that both types of nucei must compete for available vapor.

As supersaturation occurs, considerably more liquid water is absorbed by the CCN category because of the relative abundance of CCN number. The highest percentage of GCCN tends to nucleate under conditions of warmer temperature, lower CCN counts, and weaker updrafts. Nucleation of CCN within this bi-modal distribution is favored at lower temperatures and stronger updrafts. In the case where few CCN exist and the updraft is strong, the drops nucleated by both CCN and GCCN become large enough to enter directly into the cloud2 category. Examination of model results also shows that there is little variance upon the percent of nucleated CCN for any reasonable values of number concentration of CCN and GCCN that would naturally occur in the atmosphere. GCCN tend to have the greater impact when fewer CCN are present.

By assuming GCCN to be sodium chloride rather than ammonium sulfate, the solubility and density differences have the result of producing a larger equilibrium diameter, and it shifts the concentration distribution to larger sizes. The choice of a GCCN distribution with median radius of 3 microns stems from Feingold et al. (1999), where a typical median radius is given as 1-5 microns. In the present study it was found that a larger median radius of GCCN produces lower initial concentrations and less variance in the percent of GCCN that nucleate for any given value of the ambient variables, such that for increasingly large median radii, nearly all GCCN are nucleating.

Increasing the distribution breadth parameter higher than 1.8 also has the effect of decreasing the amplitude of the curve, and a decrease narrows the distribution curve while maintaining the amplitude. A value of 1.8 appears to be a sufficient balance for this application.

3. CSU-RAMS MODEL IMPROVEMENTS

Within the RAMS model microphysics the cloud2 mode was added as a new microphysics hydrometeor species with diameter from 40-80 microns. In many ways it is also an extension of the original cloud1 mode, which has a diameter up to 40 microns. Since the cloud2 mode is not considerably larger than the cloud1 mode, it has been given the same constants for mass and fall velocity calculations. Cloud2 also uses the same cloud1 mass-dependent equations for calculating the collection efficiency of droplet-ice collisions. The cloud2 droplets are considered small enough to participate in the Hallett-Mossop ice splintering process, which takes place when a super-cooled droplet contacts pristine ice, graupel, or hail in an environment with a temperature from –3C to –7C. In the condensation and evaporation processes, cloud2 droplets are influenced immediately after cloud1 droplets and before rain and the various ice phases; these are given consideration in this order due to relative competition for vapor. The cloud2 mode also participates in homogeneous freezing nucleation, which adds number and mass to the pristine ice category. Cloud2 droplets are also considered small enough that droplet temperature can be diagnosed from a heat balance equation, and they are, therefore, excluded from the internal heating calculations that rain, graupel, and hail must go through since it is possible for these three species to have relatively large amount of liquid water. Lastly, cloud2 droplets are allowed to participate in the sedimentation process, as are all the other hydrometeor species, except cloud1 droplets.

One of the largest impacts to the RAMS model due to the introduction of the cloud2 mode appears in the creation of the lookup tables of the bin representation of the collision/coalescence process involving cloud1 droplets, cloud2 droplets, and rain. The previous version of RAMS considers only collisions between: cloud1-cloud1, cloud1-rain, and rain-rain. This previous version allowed the cloud1 category to contain droplet diameters up to 80 microns. The introduction of the new mode has added three more collision considerations such that the following are all possible considerations: cloud1-cloud1, cloud1-cloud2, cloud2-cloud2, cloud1-rain, cloud2-rain, and rain-rain. The cloud2 addition has

allowed the cloud1 mode to extend to only 40 microns. The cloud2 mode takes up the 40-80 micron bins, and rain is considered larger than 80 microns. Inclusion of the cloud2 mode now requires that cloud1-cloud1 collisions must first enter the cloud2 mode instead of directly entering the rain category. Cloud1-cloud2 and Cloud2-cloud2 collisions can directly enter the rain category.

This process uses the mass doubling of bins from Tzivion(1987), which allocates 4 of 36 bins for the 40-80 micron mode. Cloud droplets that engage in the collision/coalescence process will begin growing and will be forced to enter the cloud2 category before transferring to rain. This tends to slow the growth rate into rain, and therefore delays the onset of precipitation and limits the surface accumulation of rain.

In addition to the introduction of the large droplet mode, the collection kernel from Hall (1980) has been added in order to test this against the kernel from Long (1974). It has been suspected that Long's kernel allows rain to be created too quickly in the collection process. This will have to be further tested in detail to determine if the Hall kernel helps to slow down rain production.

A collection kernel for cloud droplets colliding with snow columns (Wang, 2000) has also been manipulated to fit into RAMS bin collection process. Fully functional implementation and testing of this kernel will wait until all previous changes are proven satisfactory in different cloud-type environments. It is also desirable to have kernels available for collection of droplets with other ice species. An adaptation of the general collection efficiencies from Bohm (1992a,b,c, 1994, 1999) has been attempted but results are not yet adequate. A further look into Bohm's processes will be attempted as time permits following further testing of the second cloud mode and number concentration prediction of both cloud modes.

4. DUAL-CLOUD-MODE RESULTS

Current testing of the new microphysics with the addition of the second cloud mode and prognostic cloud number concentration has involved supercell simulations initiated with a homogeneous convective sounding and a warm bubble.

The first simulations were performed to test the effects of the basic addition of the cloud2 mode as an additional hydrometeor species. As mentioned previously it was suspected that the cloud2 mode would have the effect of slowing the onset of rainfall and limiting the rainfall amounts. The first three simulations contained CCN nucleation but not GCCN nucleation. Figure 1 displays the accumulated rain at 30min into the run. The top panel shows the accumulation in which only cloud1 exists, and in the middle panel, both cloud modes exist. Already at 30min, the very presence of the

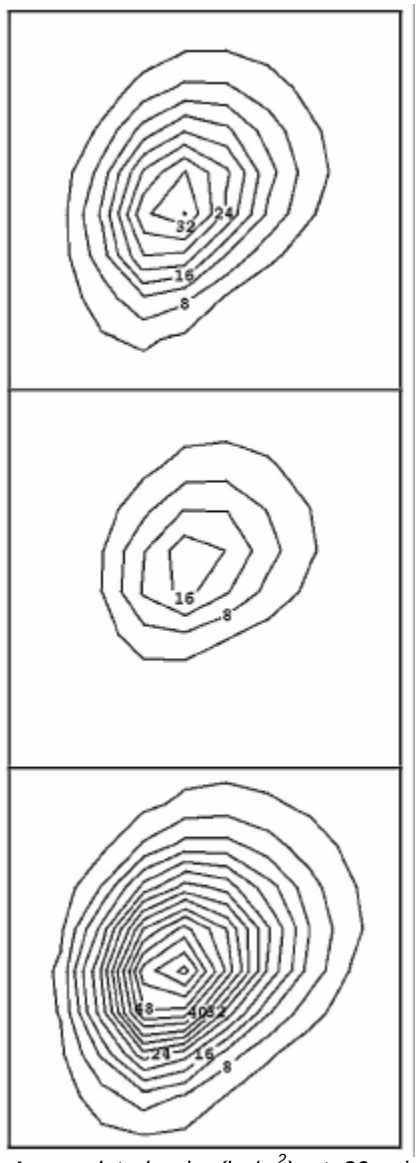

Fig. 1. Accumulated rain (kg/m^2) at 30 min into the supercell simulation with only CCN nucleated. The differences are: only cloud1 present (top), both cloud1 and cloud2 present (middle), and only cloud1 present but with depletion of CCN upon nucleation (bottom).

cloud2 mode has allowed only one-half of the rainfall compared to the single cloud mode case. This result is present at even earlier times in the simulation such that the cloud2 mode delayed the initial onset of rain.

The second set of tests allowed for nucleation of both CCN and GCCN with median radii of 0.04 and 3.0 microns, respectively; they also contained initial homogeneous CCN and GCCN fields with no source or sink terms, and both cloud modes were turned on. Test simulations were completed for various initial concentrations of CCN and GCCN. Four simulations were initialized with the following CCN and GCCN concentration pairs with units of (#/cm^3): (CCN = 900, GCCN = 10^{-5}), (CCN = 900,

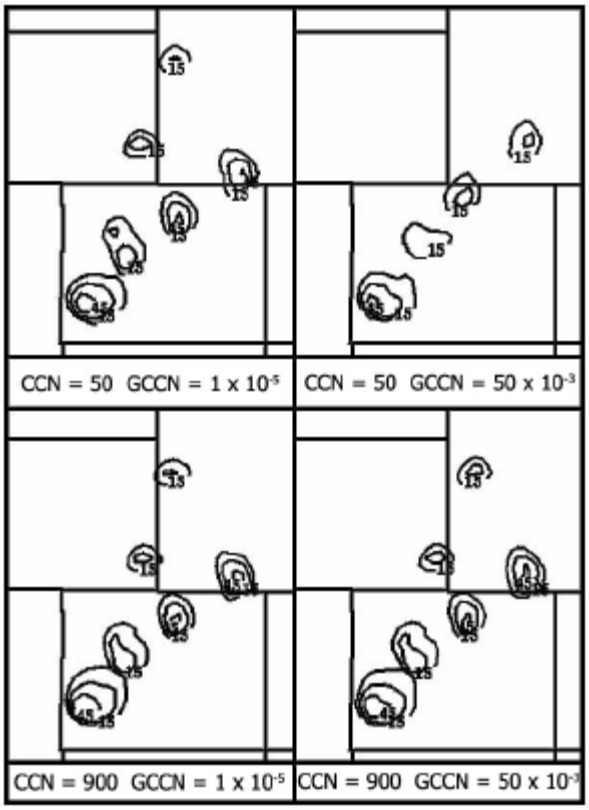

Fig. 2. Time-lapse of vertical velocity (m/s) at 9330 meters for the warm bubble simulation. Simulations are identical except for the variations in concentration of CCN and GCCN, which are given on the figure in units of (#/cm^3). Each northeastward progression of the main updraft(s) is +20 minutes of simulated time.

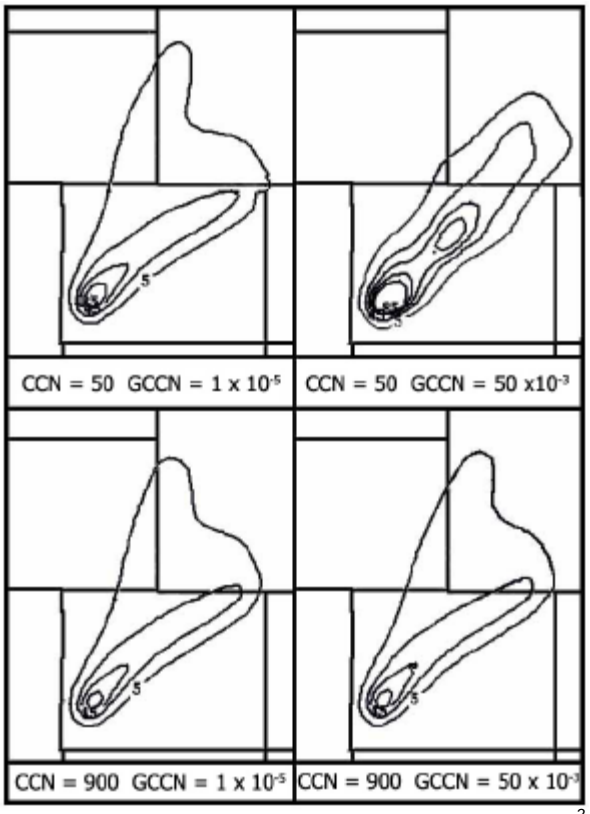

Fig. 3. Swath of accumulated rain at the surface (kg/m^2). Each contour is an increment of 20kg/m^2. Simulation initial conditions are identical except for the variations in concentration of CCN and GCCN, which are given on the figure in units of (#/cm^3).

GCCN = 50x10^{-3}), (CCN = 50, GCCN = 10^{-5}), and (CCN = 50, GCCN = 50x10^{-3}). Time lapse of the vertical velocity field at twenty-minute intervals reveals significant differences among the four simulations (Fig 2). The simulation containing fewer CCN (50) and greater GCCN (50x10^{-3}) produced a weaker central updraft at 9330 meters compared to the other simulations, and this supercell did not contain both a right and left mover.

Among the other three simulations, the differences in the updrafts are rather minor, and they mostly differ by small displacements and magnitudes. From this alone, it is evident that the most significant impact of GCCN nucleation occurs in situations in which both the number of CCN is small and the number of GCCN is large for their given range of possible values. When the number of CCN is large, any reasonable number of GCCN appears to have a lesser effect; the large number of CCN dominate the nuclei field and allow for larger water content to remain within the cloud. The influence of GCCN tends to become significant for an atmosphere in which there are few small CCN but a relative abundance of GCCN. A possible example of such a combination of nuclei may include marine environment in which airborne seasalt is prevalent and in which pollution is minimal.

Fields of total rainfall accumulation reveal that larger concentrations of CCN reduce the amount of rainfall that is produced (Fig 3). It is also shown that a significant difference in total rainfall appears as the number of GCCN is increased and CCN concentrations are kept to a minimum. The effects of GCCN nucleation become dominant over the CCN nucleation; since the GCCN nucleate directly into the large cloud2 mode, fewer total cloud droplets are produced. This allows more vapor growth of these fewer droplets up to sizes that require a transfer into the rain category. Also, as mentioned previously, collisions among cloud2 droplet directly transfer to rain since they already consist of relatively large droplets. In combination, the vapor and collisional growth processes produce more large droplets and fewer small droplets, which has the effect of producing more rain over a localized swath while inhibiting storm splitting as seen in both figures 2 and 3.

Initial tests appear promising and the model is generally behaving as expected. Further tests need to be performed for other situations, especially ones involving icing situations such as freezing rain and

freezing fog, where the second mode is likely to have a more significant impact than in the supercell simulations.

5. CCN/GCCN SOURCES AND SINKS

The incorporation of prognostic number concentration of cloud droplets into RAMS has thus far assumed a field of CCN and/or GCCN that have a constant median radius and no present sources or sinks. A variable median radius of nuclei was initially excluded from the cloud nucleation lookup tables because this would result in a 6-D table and be expensive to computational memory.

The Lagrangian parcel model revealed that nearly all of the GCCN with median radius larger than 1 micron will nucleate for any given range of temperature, vertical velocity, and number concentration that is allowed within the ranges specified earlier. Given these results, the GCCN dependence was taken out of the cloud droplet nucleation-lookup-table and the dependence of CCN nucleation on median radius was included.

This change in nucleation now requires that all GCCN nucleate prior to activation of CCN, and these GCCN will nucleate directly into the large droplet category. Once all GCCN are depleted, excess vapor can begin to nucleate the smaller CCN. Nucleation of CCN will then depend upon the ambient temperature, vertical velocity, CCN concentration, and median radius; the initial median radius is specified by the user, but this value is allowed to change with time and range between 0.01 – 0.96 microns. As CCN nucleate, the largest nuclei are activated first and removed from the available field of CCN; this will leave behind a field of CCN with a smaller median radius. Since a lesser percentage of CCN with smaller radii are activated for given atmospheric conditions, the option of having a dependency on median radius will limit the amount of cloud water that can accumulate.

CCN source and sink terms have also been included in the latest test version, though the general source terms are still being adapted. Upon nucleation of cloud droplets, the CCN number is depleted by the number that are nucleated. Available CCN mass is also depleted according to the standard log-normal distribution used in the parcel model. Lookup tables corresponding to the number of bins in the parcel model have been constructed to hold the number and mass per bin for a given concentration and median radius of CCN. Tables were created for 14 possible median radii, between 0.01 – 0.96 microns, and a number concentration of 1/cm^3. When the table is used, the present value of number concentration is multiplied by the table value in order to retrieve the amount of

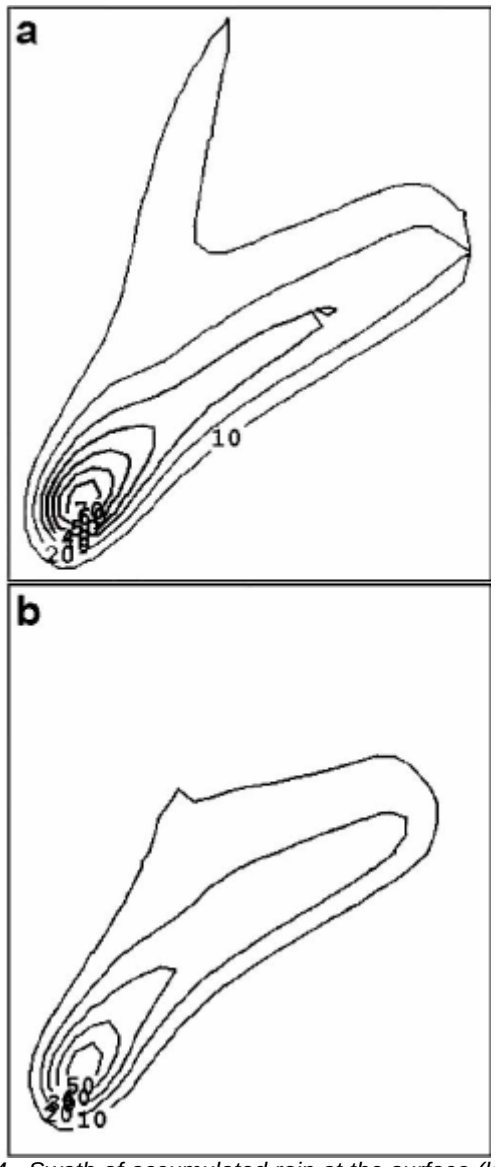

Fig. 4. Swath of accumulated rain at the surface (kg/m^2). Each contour is an increment of 10kg/m^2. Simulation initial conditions are identical except that panel (a) contains a CCN sink whereby CCN are depleted upon nucleation, and panel (b) keeps the initial CCN field constant such that there are always abundant CCN available to nucleate.

mass and number within the bin for that given median radius. By simply summing consecutive bins until the sum equals the number of nucleated CCN, it is possible to obtain the amount of nucleated mass. Due to this approach it is possible to nucleate large CCN first, deplete the largest masses according to the parcel model table, and recalculate the median radius of the remaining CCN; this will have a noticeable effect on the percentage of CCN nucleated at the following timestep.

Figure 4 displays the resulting differences in accumulated rain for the supercell simulation

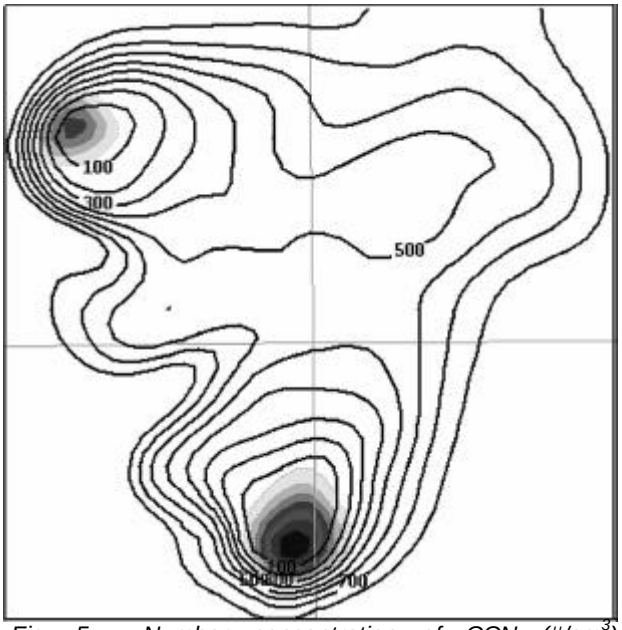

Fig. 5. Number concentration of CCN (#/cm^3) (contoured) and updraft velocity (shaded contours in 5m/s intervals) after 120 minutes of simulation time. Initial CCN concentration was 900/(cm^3).

depending upon whether or not CCN are allowed to deplete upon nucleation. The top (bottom) panel shows the swath of rainfall that accumulates by 90 minutes into the simulation with (without) depletion of CCN. By allowing CCN to be nucleated out of the available field, this limits the amount of small cloud droplets that can form, and allows for fewer droplets to continue growing to rain sizes by collection and vapor diffusion. By having a continuously available CCN field and a larger number of small droplets, any vapor growth is spread out amongst a large number concentration, such that fewer droplets can grow large enough to fall to the surface.

The effects of CCN depletion are also well portrayed by examining the correlation between the CCN concentration and the main updraft cores of the supercell simulation (Fig 5). The initial CCN concentration was a homogeneous field with 900/(cm^3). By 120 minutes into the simulation, the storm had split, and nuclei concentrations near the central updrafts had decreased to nearly 10% of the original value. Concentrations also decreased significantly in the downstream anvil region as the storm propagated to the northeast.

6. CONCLUSIONS

The CSU-RAMS model bulk-microphysics has been upgraded to include a second mode of cloud droplets that represents cloud droplets with a 40-80 micron diameter range. The inclusion of the second mode better represents the two modes that exist naturally in many environments. The large droplet mode is shown to slow the process of rain development and/or reduce the total amount of rainfall for at least a single test case involving a supercell simulation.

Accompanying this upgrade is the development of prognostic number concentration of both cloud droplet modes through the introduction of nucleation of CCN and GCCN. Nucleation of these two nuclei modes is possible via a Lagrangian parcel model that is based upon the Kohler equations. Lookup tables contain the percentage of CCN to nucleate depending upon atmospheric temperature, vertical velocity, number concentration of CCN, and the median radius of CCN. The model user has the freedom to specify the initial 3-D fields of CCN and GCCN concentration and the median radius of the nuclei. CCN sink terms exist, and the source terms are still being implemented. Once further developments are made to the source terms, a CCN mass-tracking option will be in place to include the influence of CCN restoration upon hydrometeor evaporation. It will be interesting to examine the relative amount of CCN mass contained within hydrometeor species. Given that hydrometeors may be transported far from their nucleation location, it will be possible to examine the impact of CCN loading if these displaced hydrometeors evaporate and restore large amounts of CCN in a relatively un-nucleated region.

Further test simulations will be run for various environments, including those dominated by warm and cold processes; we will examine the effects on situations dominated by liquid and/or ice phase hydrometeors.

Acknowledgments. This research was supported by a grant from the National Center for Atmospheric Research under grant 500-19852. We would like to thank Bob Walko of ATMET, Inc. for his consulting and assistance in improving the RAMS model microphysics code, and Graham Feingold of NOAA-ETL for his assistance with the Lagrangian parcel model.

7. REFERENCES

Feingold, G., and A.J. Heymsfield, 1992: Parameterizations of condensational growth of droplets for use in general circulation models. *J. Atmos. Sci.*, **49**, 2325-2342.

Feingold, G., W. Cotton, S. Kreidenweis, and J. Davis, 1999: The impact of giant cloud condensation nuclei on drizzle formation in stratocumulus: implications for cloud radiative properties. *J. Atmos. Sci.*, **56**, 4100-4117.

Kunkel, B., 1969: Comments on “A generalized equation for the solution effect in droplet growth”. *J. Atmos. Sci.*, **26**, 1344-1345.

Long, A., 1974: Solutions to the droplet collection equation for polynomial kernels. *J. Atmos. Sci.*, **31**, 1040-1052.

Pruppacher, H., and J. Klett: 1997. Microphysics of Clouds and Precipitation. Second Revised Edition. Volume 18. Kluwer Academic Publishers. Dordrecht/Boston/London. Printed in The Netherlands.

Tzivion S., G. Feingold, and Z. Levin, 1987: An efficient numerical solution to the stochastic collection equation. *J. Atmos. Sci.*, **44**, 3139-3149.

Wang, P., and W. Ji, 2000: Collision efficiencies of ice crystals at low-intermediate reynolds numbers colliding with supercooled cloud droplets: A numerical study. *J. Atmos. Sci.*, **57**, 1001-1009.